A Convolution Particle Filtering Approach for Tracking Elliptical Extended Objects

Donka Angelova*, Lyudmila Mihaylova**, Nikolay Petrov**, Amadou Gning‡
*Institute of Information and Communication Technologies, Bulgarian Academy of Sciences
Acad. G. Bonchev - 25A, Sofia, Bulgaria
Email: donka@bas.bg
**School of Computing and Communications
Lancaster University, United Kingdom
Email: mila.mihaylova@lancaster.ac.uk, n.petrov@lancaster.ac.uk
‡Department of Computer Science, University College London, United Kingdom
Email: a.gning@cs.ucl.ac.uk

***Abstract*—This paper proposes a convolution particle filtering approach for extended object tracking. Convolution particle filters (CPFs) are likelihood free filters. They are based on convolution kernel probability density representation. They use kernels to approximate the likelihood of the observations and represent the likelihood when it is analytically untractable or when the observation noise it too small. Hence, the CPFs represent a sub-family of particle filters with improved efficiency in state estimation of nonlinear dynamic systems. A CPF is designed and implemented for track maintenance of an object with an elliptical shape. The object kinematics and its extent are estimated in the presence of dense clutter. This nonparametric filter is validated with a Poisson model for the measurements, originating from the target and clutter. Simulation examples illustrate the filter performance. It is shown that the CPF yields correct estimates of the joint probability density function of the state variables and unknown static parameters. The results obtained for the extended objects show that the CPFs provides accurate on-line tracking, with satisfactory estimation of the target shape and volume.**

I. Introduction

Extended objects are characterised by a relatively large and fluctuating number of sensor reports, which originate from varying scattering centers of the object surface. The aim is to infer both the location and size of the extended object [17] based on the sequence of measurement data and available prior information [21].

Since the data often contains signals reflected from the environment (clutter) and not only from the extended target, the data association problem is much more complex than that of a conventional point target tracking. One possible solution to this problem is suggested by Gilholm and Salmond [14], [15]. They proposed a Bayesian filter for tracking an extended object based on two axiomatic assumptions: (1) the number of received target and clutter measurements at each time step are Poisson distributed (which means that several measurements can originate from the target), and (2) the target extent is modelled by a spatial probability distribution. The Poisson assumption avoids the evaluation of data association hypotheses, giving a wealth of Monte Carlo-based (particle) filter algorithms. The measurement likelihood in this type of filters is calculated as a convolution of a known object-dependent spatial distribution of measurement sources with the sensor error distribution. The likelihood computation requires integration and complicates the filter application in a number of practical situations.

The second problem of extended object tracking is related to the estimation of extent parameters. The development of efficient methods for simultaneous dealing with fixed model parameters and dynamic state variables is still a very challenging task. The unknown size and shape parameters are usually incorporated into the estimated state vector with the addition of an artificial noise. The augmented state approach (containing both the states and parameters) degrades the performance of conventional particle filters. Furthermore, the discrete nature of distribution approximations in particle filters can lead to filter divergence in a long time period [16].

The convolution particle filters (CPFs) rely on convolution kernel density estimation and regularisation of both state and observation variable distributions [26], [8], [9], [27]. They form a class of particle filters with valuable advantages: simultaneous estimation of state variables and unknown static parameters and continuous approximation of the corresponding probability density functions (PDF). Being likelihood free filters makes them attractive for solving complex problems where the likelihood is not available in an analytical form. The conditional PDF of static parameters is estimated without adding of artificial noise. The kernel and artificial noise techniques for fixed parameters evaluation are compared in [20], where the superiority of the kernel smoothing of parameters is demonstrated.

The application of CPF to extended target tracking avoids the relatively intractable calculation of the observation likelihood function and allows correct estimation of the target extent. The present paper implements one of the most efficient variants of the convolution filter, namely the resampled convolution filter [28].

The smoothing properties of kernel density approximation are applied to the task of clutter spatial intensity estimation in multiple target tracking applications in [10]. The convolution kernel approximation of the probability hypothesis density

(PHD) of the PHD filter is successfully employed for tracking of multiple targets in [22], [29]. In [2] we have implemented a CPF for tracking of a stick (rod) type of object with a uniform spatial probability distribution. The encouraging results gave us the basis for the present research.

In addition to the lack of measurements related to the object size, the main difficulty of extent estimation is the weak relationship between kinematic and shape parameters. One of the most recent, successful and widely used approach to extended object tracking [18], [13] models the object extent as a symmetric positive definite (SPD) random matrix. The ellipsoidal extension is represented by an inverse Wishart distribution. Shape parameters are estimated jointly with the state dynamics in the framework of Kalman filtering. The behaviour of group objects, including the group splitting and merging can be modeled by the SPD random matrix. Other approaches are described in [5], [4].

The aim of the present study is to design the CPF framework for tracking extended objects with elliptical and circular shapes. The object extent is modeled by a SPD non-random (constant) matrix. The major and minor semi-axes of the ellipse are treated as static parameters to be estimated by the CPF. The ellipse orientation coincides with the estimated object heading. The objective is to explore the capabilities of the convolution filters to achieve a high estimation accuracy of both state and extent parameters. The measurement sources and clutter are uniformly distributed over the whole object surface. The CPF is studied over scenarios of a nonmaneuvering and maneuvering target.

The remaining part of the paper is organised as follows. Section II formulates the problem. Section III summarises the Bayesian sequential Monte Carlo (SMC) framework. The theoretical background of the PF and CPF is described. Section IV yields in details the CPF realisation. Results for object tracking with circular and elliptical shapes are shown in Section V. The concluding remarks are given in Section VI.

II. Problem Formulation

The extended object dynamics and sensor equations are:

$$\boldsymbol{X}_k = f(\boldsymbol{X}_{k-1}, \boldsymbol{\eta}_k), \tag{1}$$

$$\boldsymbol{z}_k = h(\boldsymbol{x}_k, \boldsymbol{w}_k), \tag{2}$$

where $\boldsymbol{X}_k = \left(\boldsymbol{x}_k^T, \boldsymbol{\theta}^T\right)^T \in \mathbb{R}^{n_x+n_\theta}$, is the unknown object state vector at time k, $k \geq 1$, with T being the transpose operation. The vector $\boldsymbol{X}_k$ consists of the object kinematic state vector $\boldsymbol{x}_k \in \mathbb{R}^{n_x}$ and the object extent is described by the parameter vector $\boldsymbol{\theta}_k \in \mathbb{R}^{n_\theta}$; $f(.)$ and $h(.)$ are respectively the object and the measurement transition PDFs, $\boldsymbol{z}_k \in \mathbb{R}^{n_z}$ is the measurement vector and $\boldsymbol{\eta_k}$ and $\boldsymbol{w_k}$ are the process and measurement noises, respectively. Suppose that the initial probability density functions of $p_0(\boldsymbol{x})$ and $p_0(\boldsymbol{\theta})$ are given. Assume that at each time step k a set of sensor measurements $\boldsymbol{Z}_k = \{\boldsymbol{z}_1, \ldots, \boldsymbol{z}_{m_k}\} \in \mathbb{R}^{n_z \times m_k}$ becomes available. Each of these m_k measurements originates either from the target or from random clutter. The *goal* is to estimate, in real time, the posterior state PDF $p(\boldsymbol{X}_k|\boldsymbol{Z}_{1:k})$, given a sequence of measurement sets $\boldsymbol{Z}_{1:k} = \{\boldsymbol{Z}_1, \ldots, \boldsymbol{Z}_k\}$, collected up to time k.

III. Bayesian Sequential Estimation

The Bayesian recursive filter evaluates the posterior density by first predicting the object state

$$p(\boldsymbol{X}_k|\boldsymbol{Z}_{1:k-1}) = \int p(\boldsymbol{X}_k|\boldsymbol{X}_{k-1}) p(\boldsymbol{X}_{k-1}|\boldsymbol{Z}_{1:k-1}) d\boldsymbol{X}_{k-1} \tag{3}$$

and then updating the prediction with the information from the current set of measurements:

$$p(\boldsymbol{X}_k|\boldsymbol{Z}_{1:k}) \propto p(\boldsymbol{Z}_k|\boldsymbol{X}_k) p(\boldsymbol{X}_k|\boldsymbol{Z}_{1:k-1}). \tag{4}$$

The system dynamics PDF $p(\boldsymbol{X}_k|\boldsymbol{X}_{k-1})$ is assumed to be available from the model (1). The likelihood $p(\boldsymbol{Z}_k|\boldsymbol{X}_k)$ is specified based on (2).

A. Particle filtering

Particle filters approximate the system state PDF by a discrete set of N samples/particles with corresponding weights $\{\boldsymbol{X}_k^{(i)}, w_k^{(i)}, \quad i = 1, \ldots, N\}$. The particle set is propagated and updated by the filter according to the relationships (3)-(4). The empirical distribution given by the particles and weights is used to approximate the state posterior pdf as

$$p(\boldsymbol{X}_k|\boldsymbol{Z}_{1:k}) \approx \sum_{i=1}^{N} w_k^{(i)} \delta(\boldsymbol{X}_k - \boldsymbol{X}_k^{(i)}), \tag{5}$$

where $\delta(.)$ is the Dirac delta function, and the weights are normalised such that $\sum_i w_k^{(i)} = 1$.

B. Convolution particle filtering

The approach, proposed in [26], [8], [9] is based on the convolution kernel density estimation and regularisation of both state and observation variable distributions. The CPF relies on the following representation of the conditional state density [26]:

$$p(\boldsymbol{X}_k|\boldsymbol{Z}_{1:k}) = \frac{p(\boldsymbol{X}_k, \boldsymbol{Z}_{1:k})}{\int p(\boldsymbol{X}_k, \boldsymbol{Z}_{1:k}) d\boldsymbol{X}_k}. \tag{6}$$

Suppose, that we can sample from the state and measurement probability distribution functions, $f(.|\boldsymbol{X}_{k-1})$ and $h(.|\boldsymbol{X}_k)$, respectively. Then we can obtain a sample from the joint distribution $\{\boldsymbol{X}_k^{(i)}, \boldsymbol{Z}_k^{(i)}, \quad i = 1, \ldots, N\}$ at time step k by k successive simulations, starting from the sample of the initial distribution $p_0(\boldsymbol{X})$. Similarly to the approximation (5), we can get the following empirical estimate of the joint density

$$p(\boldsymbol{X}_k, \boldsymbol{Z}_{1:k}) \approx \frac{1}{N} \sum_{i=1}^{N} \delta(\boldsymbol{X}_k - \boldsymbol{X}_k^{(i)}, \boldsymbol{Z}_{1:k} - \boldsymbol{Z}_{1:k}^{(i)}). \tag{7}$$

The kernel estimate $p_k^N(\boldsymbol{X}_k, \boldsymbol{Z}_{1:k})$ of the true density $p(\boldsymbol{X}_k, \boldsymbol{Z}_{1:k})$ is obtained by convolution of the empirical estimate (7) with an appropriate kernel

$$p_k^N(\boldsymbol{X}_k, \boldsymbol{Z}_{1:k}) = \frac{1}{N}\sum_{i=1}^{N} K_h^X(\boldsymbol{X}_k - \boldsymbol{X}_k^{(i)}) K_h^{\bar{Z}}(\boldsymbol{Z}_{1:k} - \boldsymbol{Z}_{1:k}^{(i)}), \tag{8}$$

where $K_h^{\bar{Z}}(\boldsymbol{Z}_{1:k} - \boldsymbol{Z}_{1:k}^{(i)}) = \prod_{j=1}^{k} K_h^Z(\boldsymbol{Z}_j - \boldsymbol{Z}_j^{(i)})$ and K_h^X and K_h^Z are the Parzen-Rosenblatt kernels of appropriate dimensions. According to equation (6), the estimate of the posterior conditional state density has the following form:

$$p_k^N(\boldsymbol{X}_k|\boldsymbol{Z}_{1:k}) = \frac{\sum_{i=1}^{N} K_h^X(\boldsymbol{X}_k - \boldsymbol{X}_k^{(i)}) K_h^{\bar{Z}}(\boldsymbol{Z}_{1:k} - \boldsymbol{Z}_{1:k}^{(i)})}{\sum_{i=1}^{N} K_h^{\bar{Z}}(\boldsymbol{Z}_{1:k} - \boldsymbol{Z}_{1:k}^{(i)})}. \tag{9}$$

The convergence properties of the posterior density estimate to the optimal filter are investigated in [26], [8], [9], [28].
Since the state vector comprises both the kinematic state and the extent, equation (9) can be written in the form:

$$p_k^N(\boldsymbol{x}_k, \boldsymbol{\theta}_k|\boldsymbol{Z}_{1:k}) = \\ = \frac{\sum_{i=1}^{N} K_h^Z(\boldsymbol{Z}_k - \boldsymbol{z}_k^{(i)}) K_h^\theta(\boldsymbol{\theta}_k - \boldsymbol{\theta}_k^{(i)}) K_h^x(\boldsymbol{x}_k - \boldsymbol{x}_k^{(i)})}{\sum_{i=1}^{N} K_h^Z(\boldsymbol{Z}_k - \boldsymbol{z}_k^{(i)})}, \tag{10}$$

where $K_h^x(\boldsymbol{x}_k - \boldsymbol{x}_k^{(i)})$ and $K_h^\theta(\boldsymbol{\theta}_k - \boldsymbol{\theta}_k^{(i)})$ are the kernels for state and parameter vectors.

The main difference between the CPF and PF consists in the way the particle weights are estimated. By simulating according to the observation equation, a sample from the observation distribution is obtained. The discrete observation density is approximated with a continuous kernel density, which is used to calculate the weights in place of the likelihood function in the PF algorithm.

The implementation of the CPF requires a careful selection of several design parameters: the initial density, kernels, kernel bandwidths and number of particles. The widespread Gaussian kernel function is used in the present implementation. The choice of the kernel bandwidth is crucial, since it affects the filter convergence and accuracy of the state estimates. The theoretical considerations for the selection of kernel parameters are comprehensively presented in [24].

The kernel bandwidths are selected as follows:
1. *Choice of the bandwidth h^Z for the kernel K_h^Z.*
An automatic bandwidth selection method designed for a Gaussian kernel is proposed in [7]. The authors give also a MATLAB program for the two-dimensional data, (kde.m), with diagonal bandwidth matrix, which we employ here. The density estimate, obtained by this procedure is shown in Fig.1.

2. *Choice of bandwidths h^x and h^θ for the kernel K^X.*
The smoothing parameters are chosen according to [24], p. 87:

$$h^x = [4/(n_x+2)]^{1/(n_x+4)} N^{-1/(n_x+4)},$$
$$h^\theta = \sigma_\theta [4/(2n_\theta+1)]^{1/(n_\theta+4)} N^{-1/(n_\theta+4)},$$
$$\sigma_\theta^2 = n_\theta^{-1} \sum_{i=1}^{n_\theta} \boldsymbol{\Sigma}_\theta(ii),$$

where $\boldsymbol{\Sigma}_\theta$ is the sample covariance matrix of the parameter vector.

The resampling procedure is performed according to the scheme, proposed in [24], (pp. 143-144). The first and second moments of the resampled realisations are the same as those of the original, starting sample.

A detailed description of the CPF algorithm is given in Table 1. The estimation of the kinematic states and extent parameters is presented separately for clarity.

Table 1. The convolution particle filter for extended object tracking

I. Initialisation:
$k = 0$, $for\ \ i = 1, \ldots, N$ generate particles
$\bar{\boldsymbol{x}}_0^{(i)} \sim p_0(\boldsymbol{x})$, $\bar{\boldsymbol{\theta}}_0^{(i)} \sim p_0(\boldsymbol{\theta})$, $w_0^{(i)} = 1/N$, $k = k+1$
II. Iterate: over steps 1) to 5) for $k \geq 1$
if $k = 1$: Prediction: $for\ \ i = 1, \ldots, N$
$\boldsymbol{x}_k^{(i)} \sim f(.|\bar{\boldsymbol{x}}_0^{(i)}, \bar{\boldsymbol{\theta}}_0^{(i)})$ - state sampling
$\boldsymbol{\theta}_k^{(i)} \sim \bar{\boldsymbol{\theta}}_0^{(i)}$ - parameter sampling
$\boldsymbol{z}_k^{(i)} \sim h(.|\boldsymbol{x}_0^{(i)}, \boldsymbol{\theta}_0^{(i)})$ - observation sampling
go to step 3)
if $k > 1$:
1) Resampling: $for\ \ i = 1, \ldots, N$
$(\bar{\boldsymbol{x}}_{k-1}^{(i)}, \bar{\boldsymbol{\theta}}_{k-1}^{(i)}) \sim p_{k-1}^N(\boldsymbol{x}_{k-1}, \boldsymbol{\theta}_{k-1}|\boldsymbol{Z}_{1:k-1})$, $w_{k-1}^{(i)} = 1/N$
2) Prediction: $for\ \ i = 1, \ldots, N$
$\boldsymbol{x}_k^{(i)} \sim f(.|\bar{\boldsymbol{x}}_{k-1}^{(i)}, \bar{\boldsymbol{\theta}}_{k-1}^{(i)})$ - state sampling
$\boldsymbol{\theta}_k^{(i)} \sim \bar{\boldsymbol{\theta}}_{k-1}^{(i)}$ - parameter sampling
$\boldsymbol{z}_k^{(i)} \sim h(.|\boldsymbol{x}_{k-1}^{(i)}, \boldsymbol{\theta}_{k-1}^{(i)})$ - observation sampling
3) Weights updating: $for\ \ i = 1, \ldots, N$
$w_k^{(i)} = w_{k-1}^{(i)} \sum_{\boldsymbol{z}_k \in \boldsymbol{Z}_k} K_h^Z(\boldsymbol{z}_k - \boldsymbol{z}_k^{(i)})$,
4) Estimating the conditional densities:

$$p_k^N(\boldsymbol{x}_k, \boldsymbol{\theta}_k|\boldsymbol{Z}_{1:k}) = \frac{\sum_{i=1}^{N} w_k^{(i)} K_h^\theta(\boldsymbol{\theta}_k - \boldsymbol{\theta}_k^{(i)}) K_h^x(\boldsymbol{x}_k - \boldsymbol{x}_k^{(i)})}{\sum_{i=1}^{N} w_k^{(i)}}$$

The conditional densities of the kinematic state and extent are derived via marginalisation of the joint density

$$p_k^N(\boldsymbol{\theta}_k|\boldsymbol{Z}_{1:k}) = \frac{\sum_{i=1}^{N} w_k^{(i)} K_h^\theta(\boldsymbol{\theta}_k - \boldsymbol{\theta}_k^{(i)})}{\sum_{i=1}^{N} w_k^{(i)}}$$
$$p_k^N(\boldsymbol{x}_k|\boldsymbol{Z}_{1:k}) = \frac{\sum_{i=1}^{N} w_k^{(i)} K_h^x(\boldsymbol{x}_k - \boldsymbol{x}_k^{(i)})}{\sum_{i=1}^{N} w_k^{(i)}}$$

5) Estimating the output state and parameter vectors:

$\hat{\boldsymbol{x}}_k = \sum_{i=1}^{N} \bar{w}_k^{(i)} \boldsymbol{x}_k^{(i)}$, $\hat{\boldsymbol{\theta}}_k = \sum_{i=1}^{N} \bar{w}_k^{(i)} \boldsymbol{\theta}_k^{(i)}$
where $\bar{w}_k^{(i)}$ are the normalised weights.

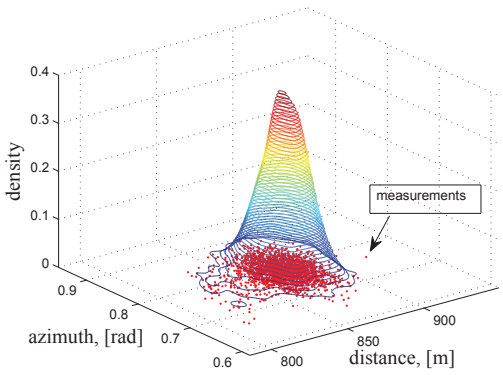

Fig. 1. Sample of the measurements and kernel density approximation of the observation distribution, obtained by MATLAB code kde.m [7]

IV. Convolution PF for Extended Object Tracking

A. Model of the Extended Target

The extended target model describes both the dynamic behaviour and spatial characteristics of the target. The selected models for nonmaneuvering and maneuvering object in 2D dimensions and its shape are described next.

Nonmaneuvering target. The temporal evolution of the target centroid in Cartesian coordinates is given by the nearly constant velocity model [3], [23]:

$$\boldsymbol{x}_k = \boldsymbol{A}\boldsymbol{x}_{k-1} + \boldsymbol{\Gamma}\boldsymbol{\eta}_{k-1}, \tag{11}$$

where $\boldsymbol{x}_k = (x_k, \dot{x}_k, y_k, \dot{y}_k)^T$ is a vector containing the position coordinates x_k, y_k, and velocities $\dot{x}_k, \dot{y}_k$, of the center of the extent;

$$\boldsymbol{A} = diag(\boldsymbol{A}_1, \boldsymbol{A}_1),\ \boldsymbol{A}_1 = \begin{pmatrix} 1 & T_s \\ 0 & 1 \end{pmatrix},$$
$$\boldsymbol{\Gamma} = \begin{pmatrix} T_s^2/2 & T_s & 0 & 0 \\ 0 & 0 & T_s^2/2 & T_s \end{pmatrix}^T,$$

T_s is the sampling interval and $\boldsymbol{\eta}_k = (\eta_x, \eta_y)_k^T$ is a discrete-time white noise sequence with components η_x and η_y, corresponding to noisy "accelerations" along x and y axes, respectively.

Maneuvering target. The object dynamics is described by a multiple-model structure with one nonmaneuvering model (11) and two coordinated turn (CT) motion models, which have (nearly) constant speed V and (nearly) constant turn rates ω. The angular rates ω are known, equal in value and opposite in sign. The state vector $\boldsymbol{x}_k = (x_k, \dot{x}_k, y_k, \dot{y}_k)^T$ is four-dimensional (as in the nonmaneuvering mode). The dynamic model with known turn rate has the following linear form [3]:

$$\boldsymbol{x}_k = \boldsymbol{B}(\boldsymbol{\omega})\boldsymbol{x}_{k-1} + \boldsymbol{\Gamma}\boldsymbol{\eta}_{k-1}, \tag{12}$$

$$\boldsymbol{B}(\boldsymbol{\omega}) = \begin{pmatrix} 1 & \sin\omega T_s/\omega & 0 & -(1-\cos\omega T_s)/\omega \\ 0 & \cos\omega T_s & 0 & -\sin\omega T_s \\ 0 & (1-\cos\omega T_s)/\omega & 1 & \sin\omega T_s/\omega \\ 0 & \sin\omega T_s & 0 & \cos\omega T_s \end{pmatrix}.$$

Since the nonmaneuvering model could be considered as a coordinated turn model with a zero turn rate ($\omega = 0$), the temporal sequence of turn rates ω_k is modeled as a Markov chain taking values from the set $\omega_i, i = 1, \ldots, M,\ (M = 3)$, with known initial $P_0(i) \triangleq P\{\omega_0 = i\}$ and transition probabilities $p_{ij} \triangleq P\{\omega_k = \omega_i | \omega_{k-1} = \omega_j\}, i, j = 1, \ldots, M$.

Target extent. The physical extension of the target is represented by a SPD constant matrix, since every positive definite matrix has a corresponding ellipsoid. An arbitrarily oriented ellipsoid is defined by

$$\text{ellipse(B)} = \{\tilde{\boldsymbol{z}} \in \mathbb{R}^{n_z} | \tilde{\boldsymbol{z}}^T \boldsymbol{B}^{-1} \tilde{\boldsymbol{z}} \leq 1\},\ \tilde{\boldsymbol{z}} = (\boldsymbol{z} - \hat{\boldsymbol{z}}), \tag{13}$$

where the center of the ellipsoid $\hat{\boldsymbol{z}}$ coincides with the predicted object position and $\boldsymbol{B}$ is a positive definite matrix. The eigenvalues of $\boldsymbol{B}$ are the squares of the semi-axis lengths. The eigenvectors of $\boldsymbol{B}$ define the semi-axis directions. The evolution model for the extent is assumed to be:

$$\boldsymbol{\theta}_k = \boldsymbol{\theta}_{k-1},\ \ \boldsymbol{\theta} = (a, \wp)^T, \tag{14}$$

where the first component of the parameter vector (a) is the major semi-axis of the ellipse and the second ($\wp = b/a$) is the aspect ratio (the ratio between the minor b and major semi-axis). The ellipse orientation φ coincides with the estimated heading: $\varphi = \arctan(\dot{y}_k, \dot{x}_k)$.

It is assumed that the aspect ratio $\wp$ takes values in the set of the following physically feasible values: $\wp \in [\underline{\wp}, \overline{\wp}]$, where $\underline{\wp} = 0.1$ and $\overline{\wp} = 1$. In the filter implementation, the aspect ratio particles are constrained inside the lower and higher set limits.
The circular shape could be considered to be a special case of elliptical shape, with equal major and minor semi-axis lengths. Then the parameter vector contains only one component which is the radius of the circle $\boldsymbol{\theta} = (r)$.

B. Measurement Generation

The measurement set $\boldsymbol{Z}_k = \{\boldsymbol{z}_1, \ldots, \boldsymbol{z}_{m_k}\}$, received from the sensor at time k originates either from the target or from random clutter. According to the Poisson model, the number of target and clutter measurements is assumed to be Poisson distributed with means λ_T and λ_C, respectively. Clutter measurements are independent of the target, while measurements from the target are distributed according to the known spatial extent model [14], [15]. The model of the spatial extent describes how measurement sources are distributed over the target surface. The PDF of a source $\boldsymbol{\xi}$, given the target state vector $\boldsymbol{x}$ can be written as $p(\boldsymbol{\xi}|\boldsymbol{x})$. In the present paper, a uniform distribution of the sources is assumed. The clutter measurements are also distributed uniformly in the observation space.

The problem of generating random points, uniformly distributed in a hyperellipsoid has different solutions, proposed in the tracking literature. Here we rely on the efficient algorithm, suggested by J. Dezert and C. Musso [11]. The MATLAB

source code, given by the authors is applied for generating measurement sources and false alarms in an ellipsoidal validation gate. The volume of the validation gate is calculated on the basis of object size and sensor errors.

C. Observation Model

Range and azimuth observations from a sensor, positioned at the beginning of the Cartesian coordinate system are considered as measurements. The measurement vector is $\boldsymbol{z}_k^j = (d_k^j, \beta_k^j)^T$, where d_k^j is the range and β_k^j is the azimuth of the measurement $j, j = 1, \ldots, m_k$. The measurement equation is of the form:

$$\boldsymbol{z}_k^j = h(\boldsymbol{\xi}_k^j) + \boldsymbol{w}_k^j, \tag{15}$$

where h is the nonlinear function

$$h(\boldsymbol{\xi}_k^j) = \left(\sqrt{\xi_{x,k}^{j2} + \xi_{y,k}^{j2}}, \tan^{-1} \frac{\xi_{y,k}^j}{\xi_{x,k}^j} \right), \tag{16}$$

$\xi_{x,k}^j$ and $\xi_{y,k}^j$ denote the Cartesian coordinates of the source point $\boldsymbol{\xi}$. The measurement noise $\boldsymbol{w}_k^j$ is supposed to be Gaussian, with a known covariance matrix $\boldsymbol{R} = diag(\sigma_d^2, \sigma_\beta^2)$.

V. Performance Evaluation

Simulation results with elliptical and circular target shape are considered to illustrate the filter performance. Root-Mean Squared Errors (RMSEs), combined on both position coordinates [3] are chosen as a measure of the algorithm accuracy. The average estimates of extent parameters also give useful information for the filter quality. In general, the estimates would be biased, and graphical results give an idea of the bias size. In the present work, a loss of track is registered, if the absolute value of position errors exceeds a threshold of 80 $[m]$ or the major semi-axis errors exceed a magnitude of 4 $[m]$. The simulation results, presented below are based on 50 Monte Carlo runs.

A. Nonmaneuvering target

The target is moving with a constant speed of $v = 10\ [m/s]$ along a heading of $-160\ [deg]$. The initial position coordinates are chosen to be equal to: $x_0 = 700\ [m]$, $y_0 = 650\ [m]$. The observer is static, located at the origin of the $(x; y)$ plane. In the case of elliptical extension, the object semi-axis lengths are $a = 40\ [m], b = 24\ [m], \wp = 0.6$ for the results, shown in the next figures. Experiments with different ellipse parameters and varying mean number of measurement sources are also fulfilled. In the circular extension, the object radius takes its values in the set $r \in \{20, 30, 40, 50\}\ [m]$.

The sensor parameters are similar to that of [6], [25]: the sampling interval is $T_s = 1\ [s]$, the measurement error standard deviations along range and azimuth are respectively 2 $[m]$ and 1.0 $[deg]$. The initial estimate of the target state is a Gaussian perturbation about the truth with zero mean and covariance matrix $\boldsymbol{P}_0^x = diag\{30^2m^2, 1.5^2m^2/s^2, 30^2m^2, 1.5^2m^2/s^2\}$ for kinematic state and $\boldsymbol{P}_0^\theta = diag\{5.0^2m^2, 0.3\}$ for the extent. The standard deviation of the acceleration noise $\boldsymbol{\eta}$ is

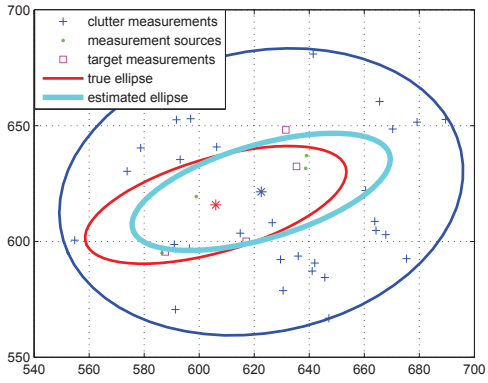

Fig. 2. Single run: true and estimated target position and shape at $k = 10$, $\lambda_T = 5$, $(\rho_{fa} = 1.0e-03)$. The validation gate is shown by a blue ellipse

$\sigma_{\dot{x}} = \sigma_{\dot{x}} = 1.4\ [m/s^2]$. The mean number of measurement sources is selected as $\lambda_T = 5$. Clutter measurements are created uniformly in an elliptical validation region, centered at the predicted object position and oriented according to the predicted heading. The validation gate, true and estimated elliptical shapes and two types of measurements - from target and clutter are given in Fig.2. The major and minor semi-axis of the validation gate are $1.5a$ and $3b$, respectively. The larger minor semi-axis accounts for comparable large azimuth sensor errors. The mean number of clutter measurements per frame is $\lambda_C = \rho_{fa}V$, where V is the volume of the validation gate. The clutter density ρ_{fa} takes values among the set $\rho_{fa} \in \{0.5e-03; 1.0e-03; 2.0e-03; 2.5e-03\}$. The number of particles is $N = 2000$.

Results with ellipsoidal object extension. The average major semi-axis estimate and its true value are presented in Fig. 3. The filter easily and accurately estimates the major semi-axis for clutter density up to $\rho_{fa} = 2.0e-03$. For higher clutter intensity ($\rho_{fa} = 2.5e-03$) the bias in estimating the axis length increases as it can be seen from Fig. 3, and 8% of the realisations lead to filter divergence. The aspect ratio and major semi-axis RMSEs are shown in Fig. 4 and Fig. 5. The maximum major semi-axis RMSEs are in the order of 2.0 $[m]$. The accuracy of the kinematic state estimates depends on the position of the object with respect to the sensor and clutter density. Position RMSEs for the selected set of clutter densities are shown in Fig. 6. Within the explored area of $\pm 800\ [m]$ around the sensor and selected ρ_{fa}, the maximum values of position and speed RMSEs are not greater than 30 $[m]$ and 3.0 $[m/s]$, respectively. RMSEs increase with the increase of clutter density. Higher levels of the clutter ($\rho_{fa} \geq 3.0e-03$) lead to larger position errors and respectively to filter degeneracy.

The results with circular object extension are given in Figs. 7, 8 and 9. The set of radii $r \in \{20, 30, 40, 50\}[m]$ corresponds to different densities of measurement sources: $\rho_T \in \{4.0e-03, 1.8e-03, 0.1e-03, 6.4e-04\}$. It is natural to expect that

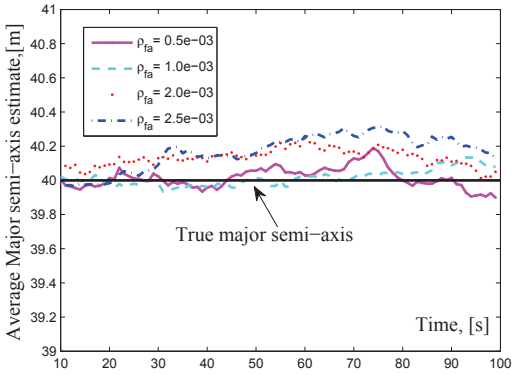

Fig. 3. Average major semi-axis estimate and its true value $a = 40m, \lambda_T = 5$

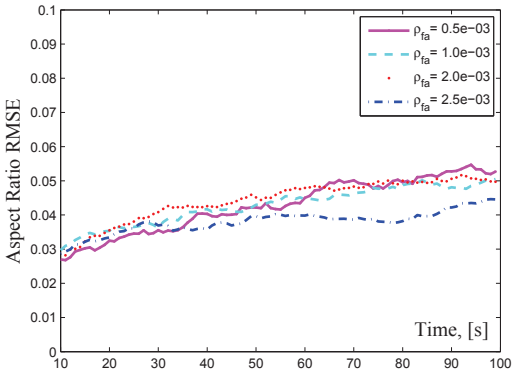

Fig. 4. Aspect ratio ($\wp$) Root Mean Square Errors, $\lambda_T = 5$.

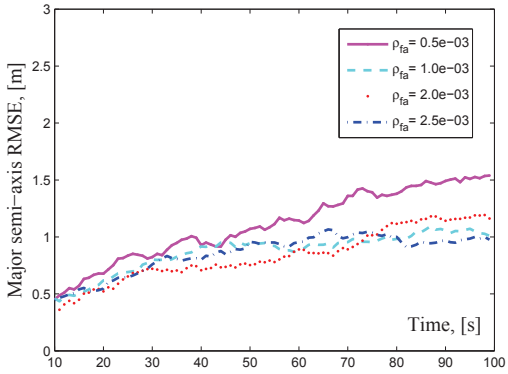

Fig. 5. Major semi-axis (a) Root Mean Square Errors, $\lambda_T = 5$.

the filter performance could be better for a larger number of target measurements. The radius RMSEs are shown in Fig. 7 for $r \in \{20, 30, 40\}$ and clutter density $\rho_{fa} = 1.0e-03$. The radius of 50 m leads to filter divergence in more than 50% of Monte Carlo realisations. Speed and position RMSEs, presented in Figs. 8 and 9 show that acceptable results could be obtained with the combination of mean number of target measurement $\lambda_T = 5$ and clutter density $\rho_{fa} = 1.0e-03$. Decreasing the mean number of target measurements leads to a loss of tracks.

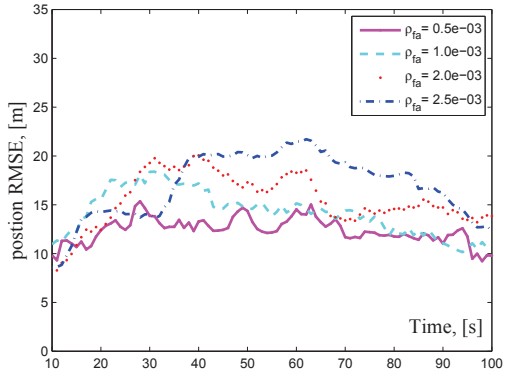

Fig. 6. Position Root Mean Square Errors

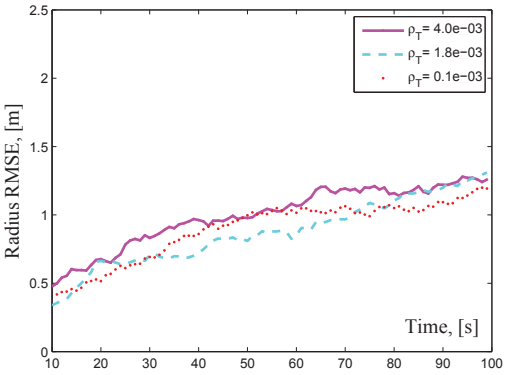

Fig. 7. Radius Root Mean Square Errors, ($\rho_{fa} = 1.0e-03$).

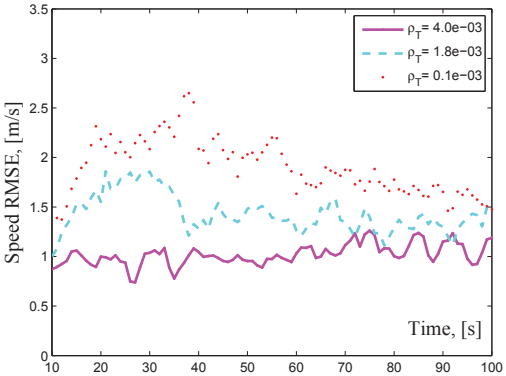

Fig. 8. Speed Root Mean Square Errors, ($\rho_{fa} = 1.0e-03$).

B. *Maneuvering target*

In the maneuvering target scenario, the object is moving with a constant speed of 10 $[m/s]$ and implements three consecutive CT maneuvers with normal accelerations $a_n = -2,\ 2$ and -1 $[m/s^2]$. This set of normal accelerations corresponds to angular rates of $\omega = \pm 0.2$ $[s^{-1}]$ and

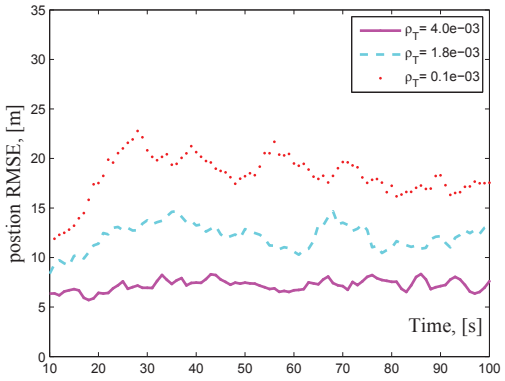

Fig. 9. Position Root Mean Square Errors, ($\rho_{fa} = 1.0e-03$).

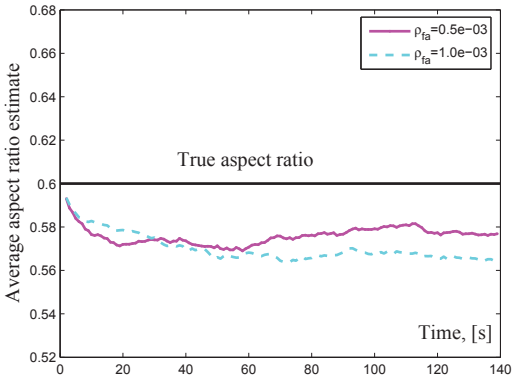

Fig. 11. Average aspect ratio estimate and its actual value

,

$\omega = -0.1$ $[s^{-1}]$. ($\pm\omega$ corresponds to left and right turn, respectively). The simulated (actual) and estimated trajectories of the target in a single run are shown in Fig. 10. Initial

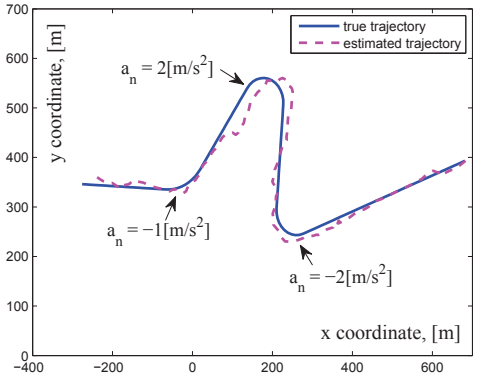

Fig. 10. Single run. True and estimated trajectory, $\rho_{fa} = 0.5e-03$

and transition mode probabilities of the underlying Markov chain are as follows: $P_0(1) = 0.6$, $P_0(2) = P_0(3) = 0.2$; $p_{11} = 0.7$, $p_{12} = 0.15$, $p_{13} = 0.15$; $p_{21} = p_{31} = 0.15$, $p_{22} = p_{33} = 0.8$, $p_{23} = p_{32} = 0.05$. The true major and minor semi-axes of the ellipse are selected as $a = 40$ and $b = 24$ $[m]$, respectively. The average aspect ratio estimate for two different clutter densities ($\rho_{fa} = 0.5e-03$ and $1.0e-03$) is presented in Fig. 11.

The position and speed RMSE, shown in Figs. 12 and 13 are calculated by removing the realisations with loss of tracks. The maximum RMS errors of the major semiaxis are not greater than 2 $[m]$. The obtained percentage of lost tracks is presented in Table 2. The acceptable tracking results are achieved for clutter densities up to $\rho_{fa} = 0.5e-03$. The percentage of the realisations with filter divergence rapidly grew for larger clutter levels.

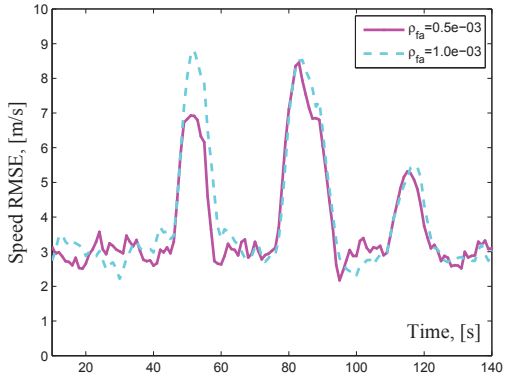

Fig. 12. Maneuvering target. Speed RMS Errors

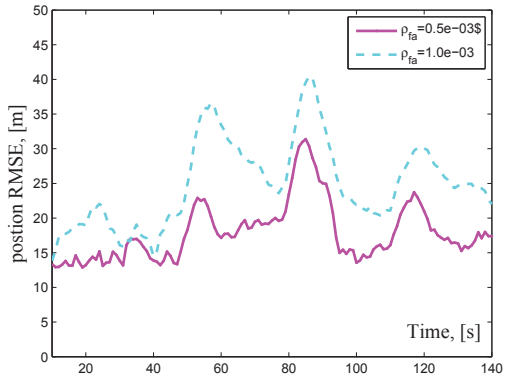

Fig. 13. Maneuvering target. Position RMS Errors

Table 2. Percentage of Lost Tracks

$\lambda_T = 5$		
$\rho_{fa} = 0.5e-03$	$\rho_{fa} = 1.0e-03$	$\rho_{fa} = 1.5e-03$
4.0	16.0	50.0

The average computational time for one iteration of the filter with 2000 particles is approximately $0.39[s]$ ($\rho_{fa} = 1.0e-03$) using a 4.7 GHz Intel CORE'I7 processor

and with MATLAB implementation. The CPF execution time is comparable with that of the conventional PF.

An important advantage of the CP filter is that an analytical form of the output state and parameter densities can be obtained, together with their point estimates. The filter disadvantage is related with the choice of the design parameters. The selection of the bandwidth is of primary importance in the CPF implementation. For the case of two dimensional measurement vector we implemented a MATLAB procedure, published in the literature. If the dimension of the measurement vector increases, the bandwidth selection could be a more serious problem.

VI. Conclusions

A convolution particle filter framework for tracking extended objects with elliptical shape is proposed in this paper. The physical extension is modeled by a symmetric positive definite non-random matrix, which defines an elliptical object shape. The object size parameters and its volume are estimated on-line, simultaneously with target dynamics. The filter performance is validated over the Poisson model of the measurements, originating from the target and clutter. The measurement sources and clutter are uniformly distributed over the whole object surface.

Simulation examples with a set of different clutter densities illustrate the filter performance. The tracking algorithm provides a good estimation accuracy for clutter intensities up to $\rho_{fa} = 2.5e-03$ and $\rho_{fa} = 0.5e-03$ for nonmaneuvering and maneuvering targets, respectively. The higher clutter densities lead to increased estimation errors and filter divergence.
The current work is focused on estimating also the clutter parameters and other approaches such as box particle filtering. The important practical case of measurement sources, uniformly located over the arc is also considered.

Acknowledgements. We acknowledge the support from the [European Community] Seventh Framework Programme [FP7/2007- 2013] under grant agreement No 238710 (Monte Carlo based Innovative Management and Processing for an Unrivalled Leap in Sensor Exploitation), MC IMPULSE and from the project AComIn "Advanced Computing for Innovation", grant 316087, funded by the FP7 Capacity Programme (Research Potential of Convergence Regions).

References

[1] P. J. Acklam, Monte Carlo Methods in State Space Estimation, Cand. Scient. Thesis, University of Oslo, 1996.

[2] D. Angelova, L. Mihaylova, N. Petrov and A. Gning, Extended Object Tracking with Convolution Particle Filtering, *Proc. of the IEEE 6th International Conf. on Intelligent Systems*, Bulgaria, 2012, pp. 96-101.

[3] Y. Bar-Shalom and X. Li, *Estimation and Tracking: Principles, Techniques and Software*. Artech House, 1993.

[4] M. Baum, Benjamin Noack, Uwe D. Hanebeck, Extended Object and Group Tracking with Elliptic Random Hypersurface Models, *Proceedings of the 13th International Conference on Information Fusion*, Edinburgh, United Kingdom, July, 2010.

[5] M. Baum, F. Faion, U. D. Hanebeck, Modeling the Target Extent with Multiplicative Noise, *Proceedings of the 15th International Conference on Information Fusion*, Singapore, July, 2012.

[6] Y. Boers, H. Driessen, J. Torstensson, M. Trieb, R. Karlsson and F. Gustafsson, A Track Before Detect Algorithm for Tracking Extended Targets, *IEE Proc. - Radar, Sonar, Navig.*, Vol. 153, No. 4, 2006.

[7] Z. Botev, J. Grotowski, D. Kroese, Kernel density estimation via diffusion, *Annals of Statistics*, Vol. 38, No. 5, pp. 2916-2957, 2010.

[8] F. Campillo, V. Rossi, Convolution Particle Filtering for Parameter Estimation in General State-Space Models, INRIA, Technical Report 5939, June, 2006 (https://hal.inria.fr/inria-00081956)

[9] F. Campillo and V. Rossi, Convolution Particle Filter for Parameter Estimation in General State-Space Models, *IEEE Transactions on Aerospace and Electronic Systems*, Vol. 45, No. 3, 2009, pp. 1063-1072.

[10] X. Chen, R. Tharmarasa, T. Kirubarajan, M. Pelletier, Online Clutter Estimation Using a Gaussian Kernel Density Estimator for Target Tracking, *Proc. of the 14th International Conference on Information Fusion*, 2011, pp. 1317-1324.

[11] J. Dezert, C. Musso, An Efficient Method for Generation Points Uniformly Distributed in Hyper-ellipsoids, *Proc. of the Workshop on Estimation, Tracking and Fusion: A Tribute to Yaakov Bar-Shalom*, Monterey, California, May 17,2001.

[12] A. Doucet, N. de Freites and N. Gordon (Eds.), *Sequential Monte Carlo Methods in Practice*, New York, Springer, 2001.

[13] M. Feldmann, D. Frnken, and W. Koch, Tracking of Extended Objects and Group Targets Using Random Matrices,*IEEE Trans. on Signal processing*, Vol.59, No.4,2011.

[14] K. Gilholm and D. Salmond, Spatial Distribution Model for Tracking Extended Objects, *IEE Proceedings on Radar, Sonar and Navigation*, Vol. 152, No. 5, pp. 364-371, 2005.

[15] K. Gilholm, S. Maskell, D. Salmond, S. Godsill, Poisson Models for Extended Target and Group Tracking, *Proc. SPIE Conference 5913: Signal and Data Processing of Small Targets*, 2005.

[16] M. Hurzeler and H. R. Kunsch, Monte Carlo Approximations for General State-Space Models, *Journal of Computational and Graphical Statistics*, Vol. 7, No. 2, 1998, pp. 175-193.

[17] W. Koch, R. Saul, A Bayesian approach to extended object tracking and tracking of loosely structured target groups, *Proc. of the 8th International Conference on Information Fusion*, 2005.

[18] W. Koch, M. Feldmann, Cluster Tracking Under Kinematical Constraints Using Random Matrices, *Robotics and Autonomous Systems*, Vol. 57, 2009 pp. 296-309.

[19] Q. Lin, J. Yin, J. Zhang, Bo Hu, Gaussian Convolution Filter and its Application to Tracking, *Wireless Sensor Networks*, Vol.1, No. 2, 2009.

[20] J. Liu, M. West, Combined parameter and state estimation in simulation-based filtering, in *Sequential Monte Carlo Methods in Practice*, Eds.: A. Doucet, N. de Freites and N. Gordon, Springer, 2001, pp. 247-271.

[21] R. Mahler, PHD Filters for Nonstandard Targets, I: Extended Targets, *Proc. of the 12th International Conf. on Information Fusion*, Seattle, WA, USA, July 6-9, 2009.

[22] K. Panta, B.-N. Vo, Convolution Kernels based Sequential Monte Carlo Approximation of the Probability Hypothesis Density (PHD) Filter, *Proceedings of the Information, Decision and Control Conference, IDS'07*, Adelaide, Australia, 2007, pp. 336-341.

[23] N. Petrov, L. Mihaylova, A. Gning, D. Angelova, A Novel Sequential Monte Carlo Approach for Extended Object Tracking Based on Border Parameterisation, *Proc. of the 14th International Conference on Information Fusion, Chicago*, USA, 5-7 July, 2011 pp. 306-313.

[24] B. W. Silverman, *Density Estimation for Statistics and Data Analysis*, Chapman & Hall, New York, 1986

[25] B. Ristic, A. Gning, L. Mihaylova, Nonlinear filtering using measurements affected by stochastic, set-theoretic and association uncertainty, *Proc. of the 14th International Conf. on Information Fusion*, 2011, pp. 1069-1076.

[26] V. Rossi, J. P. Vila, Nonlinear Filter in Discreet Time: A Particle Convolution Approach, Biostatic Group of Monetepellier, Technical Report 04-03, 2004 (http://vrossi.free.fr/recherche.html).

[27] V. Rossi and J.-P. Vila, *Annales de l'Institut de Statistique de l'Université*, Vol. 50, No. 3, Nonlinear Filtering in Discrete Time: A Particle Convolution Approach, 2006, pp. 71-102.

[28] J.-P. Vila, Enhanced consistency of the Resampled Convolution Particle Filter, *Statistics and Probability Letters*, 82(4), 2012, pp. 786-797.

[29] J. Yin, D. Zhang, J. Zhang, The Gaussian Sum Convolution PHD Filtering Algorithms for Nonlinear Models, *Information Technology Journal*, Vol. 10, No. 12, 2011, pp. 2357-2363.